JULY 1980

PPPL-1683
UC-20g

X-RAY HEATING AND IONIZATION OF BROAD-EMISSION-LINE REGIONS IN QSO's AND ACTIVE GALAXIES

BY

J. C. WEISHEIT, G. A. SHIELDS,
AND C. B. TARTER

PLASMA PHYSICS LABORATORY

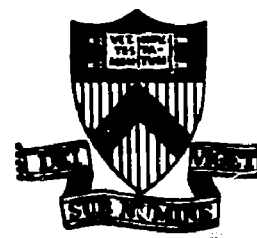

PRINCETON UNIVERSITY
PRINCETON, NEW JERSEY

This work was supported by the U.S. Department of Energy Contract No. DE-AC02-76-CHO 3073. Reproduction, translation, publication, use and disposal, in whole or in part, by or for the United States government is permitted.

X-Ray Heating and Ionization of Broad-Emission-Line Regions in QSO's and Active Galaxies

J. C. Weisheit,[1] G. A. Shields,[2] and C. B. Tarter[3]

ABSTRACT

Absorption of X-rays deep within the broad-line emitting clouds in QSO's and the nuclei of active galaxies creates extensive zones of warm ($T \sim 10^4$K), partially ionized ($N_e/N \sim 0.1$) gas. Because Lyman alpha photons are trapped in these regions, the X-ray energy is efficiently channeled into Balmer lines collisionally excited from the $n = 2$ level. These HII regions plus the HII regions created by ultraviolet photons illuminating the surfaces of the clouds give rise to integrated I_α/H_α line emission ratios between 1 and 2. Enhanced MgII line emission from the HI regions gives rise to integrated MgII/H_α ratios near 0.5. The OI line λ8446 is efficiently pumped by trapped L_α photons and in the X-ray heated zone we calculate an intensity ratio $I(\lambda 8446)/I(H\alpha) \leq 0.1$. All of these computed ratios now are in agreement with observations.

[1]Plasma Physics Laboratory, Princeton University
[2]Alfred P. Sloan Research Fellow, Department of Astronomy, University of Texas at Austin.
[3]Lawrence Livermore Laboratory, University of California.

I. INTRODUCTION

From optical data for QSO's with very different redshifts, Baldwin (1977) constructed a composite emission-line spectrum covering the range λλ1000 - 7000. He concluded that the hydrogen line intensity ratio $I(L\alpha)/I(H\beta)$ is between 3 and 6, or about an order of magnitude less than the value expected for the case of a pure recombination spectrum with optically thick Lyman lines (viz., case B). This prediction or its equivalent, $I(L\alpha)/I(H\alpha) \sim 1$, subsequently has been confirmed with spectrally extended observations of four QSO's. Type 1 Seyferts and N - galaxies now are known to exhibit anomalously low Lyman/Balmer line intensity ratios too (cf. Davidsen, 1979). The published ratios for QSO's and active galactic nuclei (AGN) having broad emission lines are given in Table 1, together with other relevant spectral properties. Also listed are mean values for QSO's and AGN, as determined from a much larger sample of objects in each class.

The different entries in this table collectively suggest that there is nothing atypical about the specific objects for which Lyman/Balmer line ratios have so far been determined (see also Canizares, McClintock, and Ricker, 1978), and that these observed quantities are quite similar for QSO's and AGN with broad-emission-line regions (BLR). Of particular interest are the large luminosities L_{xr} in the kilovolt X-ray region; recent satellite observations reveal that such large X-ray fluxes are commonplace (Tananbaum et al., 1979; Elvis et al., 1978). We have investigated the influence of the

X-radiation on the thermal and ionization structure of the BLR. A preliminary report was given by Shields (1979). In this paper we describe detailed numerical calculations which show that standard photoionization models, when extended to include kilovolt X-rays, yield hydrogen emission spectra that are in harmony with the data. In Section II we summarize the relevant atomic processes; in Section III we present numerical results; and in Section IV we discuss our calculations vis-a-vis other recent work on this subject.

II. INTERACTION OF X-RADIATION WITH BLR GAS

A. Parameters of the problem

A thorough discussion of many properties deduced for line-emitting regions in QSO's and AGN has been given by Davidson and Netzer (1979). Briefly, it is believed that the widths of broad lines are due to large dispersions in velocity ($\Delta v/c \gtrsim 10^{-3}$) among numerous clouds that have a small covering factor, $(\Omega_{BLR}/4\pi) \sim 0.1$, as viewed from the central object. The absence of broad forbidden lines and the presence of a broad CIII intercombination line together imply a high gas density within each cloud, $10^8 \leqslant N(cm^{-3}) \leqslant 10^{10}$. Instances of detected absorption of X-rays with energies $h\nu \lesssim$ few keV indicate that the total column of material in a BLR cloud is $N = \int N\, d\ell \sim 10^{21-23} cm^{-2}$, from which it follows that the cloud thickness $\ell \sim 10^{13}$cm. Optical observations of high redshift QSO's reveal power-law photon fluxes near the Lyman continuum limit

($\nu = \nu_H$), $f_\nu \sim \nu^{-\alpha_{uv}}$ with uv spectral indices in the range $0.5 \leq \alpha_{uv} \leq 1.5$.

When these parameters are used in photoionization models of QSO's and AGN (e.g., Shields, 1976; Davidson, 1977; Shuder and MacAlpine, 1979), it is found that at the surfaces of BLR clouds the ionizing flux needs to be

$$\phi_{uv} \equiv \int_{\nu_H}^{30\nu_H} (f_\nu/h\nu)\, d\nu \approx 10^{-2}\ Nc\ (\text{photons/cm}^2\ \text{s}) \qquad (1)$$

in order for the models to reproduce important ultraviolet spectral features.

The X-ray fluxes of QSO's and AGN also exhibit power-law behavior, with spectral indices $\alpha_{xr} \sim 1/2$ (cf. Stark, Burnell, and Culhane, 1978; Mushotzky et al., 1980; Tananbaum et al., 1979). However, the magnitudes of the X-ray fluxes are less than values obtained by straightforward extrapolation of the ultraviolet fluxes, and to a good approximation the number flux of X-ray photons is given in terms of the luminosity ratio L_{xr}/L_{opt} (cf., Table I) as

$$\phi_{xr} \equiv \int_{(0.5\text{keV})}^{(5\ \text{keV})} (f_\nu/h\nu)\, d\nu \approx 0.02\ \phi_{uv}[L_{xr}/L_{opt}]. \qquad (2)$$

(The integration range has been chosen to nearly coincide with the range of the IPC detector aboard the Einstein satellite.)

In order to estimate various quantities discussed in the remainder of this section, we shall adopt the numerical values $N = 3 \times 10^9 \text{cm}^{-3}$ and $L_{xr}/L_{opt} = 1/2$. These numbers yield

$\phi_{uv} = 10^{18} cm^{-2}\ s^{-1}$ and $\phi_{xr} = 10^{16}\ cm^{-2}\ s^{-1}$, and fix the typical distance of a BLR cloud from its continuum source at $d_o \simeq 2(L_{opt}/10^{46} erg\ s^{-1})^{1/2} pc$.

B. Hydrogen ionization equilibrium

In a BLR cloud, the depth ℓ_{uv} to which ultraviolet photons can keep hydrogen mostly ionized is given by the familiar photon counting estimate,

$$\ell_{uv} \simeq \phi_{uv}/N^2\beta_H \sim 10^{11.5} cm, \tag{3}$$

where $\beta_H \simeq 10^{-12.6} cm^3\ s^{-1}$ is the effective rate coefficient for hydrogen recombination at a temperature $T \sim 10^4$ K.

For a gas with normal cosmic abundances, the mean X-ray ionization cross section per H atom is (cf., Brown and Gould, 1970)

$$\langle \sigma_{xr} \rangle = \left[\int_{xr} (f_\nu/h\nu)\sigma(\nu)\, d\nu\right] \Big/ \phi_{xr} = 10^{-21.5} cm^2, \tag{4}$$

Kilovolt X-rays penetrate a BLR cloud to a depth

$$\ell_{xr} = [N\sigma(\nu)]^{-1} \simeq 10^{12} (h\nu/1\ keV)^3 cm, \tag{5}$$

and then deposit their energy in its predominantly neutral interior. Almost all of the photoabsorptions represented in Eq. (4) are K- or L-shell ionizations of heavy elements and, on average, each ionization yields an additional 1.3 electrons

due to Auger processes (Weisheit, 1974). In a partially ionized gas, the metal ions are neutralized predominantly by charge-exchange collisions with H atoms, since these reactions proceed faster than radiative (or dielectronic) recombination when $10^2 \leq T(K) \leq 10^4$ (see, for instance, Butler, Bender, and Dalgarno, 1979; Watson and Christensen, 1979; McCarroll and Valiron, 1976). Therefore, it follows that the effective hydrogen X-ray ionization probability per unit time is

$$\Gamma_H(xr) = 2.3 < \sigma_{xr} > \phi_{xr} = 10^{-5.1} \ s^{-1} \ . \tag{6}$$

An additional number Ψ of secondary hydrogen ionizations are caused by the fast Auger and photo-electrons, which initially have a total energy E_o almost as large as that of the absorbed X-ray. The thermalization of energetic electrons in a partially ionized hydrogen gas has been studied by several authors (e.g., Spitzer and Scott, 1969; Habing and Goldsmith, 1971; Bergeron and Collin-Souffrin, 1973; Shull, 1979). The tabulated results of Bergeron and Collin-Souffrin can be fitted adequately for our purposes by the expression

$$(E_o/h\nu_H)^{-1}\Psi(x,E_o) = \psi(x) = \begin{cases} 0.40, & x \leq 0.01 \\ 0.40 - 0.087 \ \ell n(100\ x), & x > 0.01, \end{cases} \tag{7}$$

where $x = N_e/N$ is the fractional ionization of the gas. This formula yields, for secondary-electron ionization of hydrogen, the probability per unit time

$$\Gamma_H(e^-) \approx 50 < \sigma_{xr} > \phi_{xr}\psi(x), \tag{8}$$

due to X-rays in the range 0.5 - 5 keV.

Upon collecting results, we find that the characteristic ionization fraction of hydrogen in the X-ray absorbing region is given approximately by the equation*

$$\frac{x^2}{1-x} = \frac{[2.3 + 50\psi(x)] < \sigma_{xr} > \phi_{xr}}{N\beta_H}, \tag{9}$$

whose solution for our specific set of parameters is $x \approx 0.2$. We expect heavier elements to be predominantly in the forms He^o, C^+, O^o, Mg^+, Fe^+, etc., subject to present uncertainties in various charge transfer rate coefficients.

C. Thermal equilibrium

According to Bergeron and Collin-Souffrin (1973), the heating efficiency of fast electrons in a hydrogen gas is

$$\xi_h \approx 1 - 2\psi(x). \tag{10}$$

---

*The true fractional ionization in BLR clouds is somewhat higher than the value given by Eq. (9) because very large Lα optical depths maintain a significant number of H atoms in the n = 2 state, which is susceptible to ionization by the large flux of continuum photons with energies $h\nu > h\nu_H/4$ (cf., Kwan and Krolik, 1979). We discuss this point in Sec. IV.

(This result can by derived from first principles if one uses the Bethe approximation to estimate the excitation and ionization cross sections.) In addition, much of the energy lost in inelastic e^- - H collisions leads to the production of Lα photons, and the energy of some of these is converted to heat via collisional deactivation of excited, n = 2, H atoms. Thus, for example, in a weakly ionized gas (x ~ 0.1) about 1/3 of the energy of absorbed X-rays is used to excite and ionize the gas, and about 2/3 is used to balance energy lost from the cloud in line and continuum radiation.

Simple estimates show that the cooling predominantly is due to Lα and to Balmer line radiation collisionally excited from the n = 2 level. There also are important contributions from the thermal excitation of allowed Fe^+ and Mg^+ lines, but, of course, fine-structure and optical forbidden line radiations are collisionally suppressed in this high electron density environment. Because excitation potentials of several eV are involved, the temperature is regulated at a value near 10^4 K. These qualitative statements are borne out by computer calculations described in Sec. III.

D. Hydrogen line intensities

Numerous authors, including Krolik and McKee (1978), Ferland and Netzer (1979), Kwan and Krolik (1979), and Canfield and Puetter (1980), have investigated hydrogen line emission from BLR clouds. Here, we give only a summary of the processes included in our numerical calculations.

We employed depth-dependent escape probabilities to determine the effects of very large Lyman-line optical depths on integrated BLR emission spectra. Let P_{nm} be the probability that a photon arising in the atomic transition $n \rightarrow m$ eventually is emitted from the cloud after a mean number of scatterings $\langle s \rangle$. If q_{nm} is the likelihood, per scattering event, that the radiative transition $n \rightarrow m$ does <u>not</u> occur, we have

$$P_{nm} = (1 - q_{nm})^{\langle s \rangle} \longrightarrow \exp(-q_{nm}\langle s_n \rangle), \tag{11}$$

with the exponential form being correct in the limits ($\langle s \rangle >> 1$, $q_{nm} << 1$). For large optical depths τ_o at line center, it has been shown (cf., Ferland and Netzer, 1979; Otsuka, 1979) that the mean number of scatterings of Lyman line photons is

$$\langle s \rangle = \frac{1.11\tau_o^{1.107}}{1 + [(\log_{10}\tau_o)/5.5]^5} \sim \tau_o, \tag{12}$$

whereas for all other (much less thick) lines $\langle s \rangle \sim \tau_o^{1/2}$.

In the context of the escape probability formalism, the occurrence of a large Lα optical depth τ_{21} does not result in the formation of any "new" atoms in the level $n = 2$; hence the Lα emission coefficient is just

$$4\pi j_{21}(\tau_{21}) = 4\pi j_{21}\ (0)\ P_{21}\ (\tau_{21}). \tag{13}$$

On the other hand, when $\tau_{21} \gg 1$ the levels $n \geq 3$ are efficiently pumped by electron impact excitations of atoms in the $n = 2$ level, at the rate $N_2 N_e k_{2n}$, in addition to the population mechanisms that operate at low optical depths. Thus, for example, the Hα line emission coefficient is

$$4\pi j_{32}(\tau_{21}) = 4\pi j_{32}(0)\left[1 + \frac{N_2 k_{23}}{N_e \beta_3 + N_1 k_{13}}\right] P_{32}(\tau_{32}), \qquad (14)$$

where $N_e \beta_3$ is the effective radiative recombination rate for the production of Hα. (Note that the branching ratio for Hα/Lα does not appear in the denominator of this equation because we are relating $j_{32}(\tau_{21})$ to the case B limit of the Hα line intensity, including collisions from ground-state H atoms.)

Emission lines' strengths can be determined from equations such as (13) and (14) as a function of the local Lα optical depth, once the $n = 2$ population is known. The quotient

$$J_{a,b}(\tau_{21}) = \int_0^{\ell(\tau_{21})} j_a(\tau)\, d\ell \Big/ \int_0^{\ell(\tau_{21})} j_b(\tau)\, d\ell \qquad (15)$$

then gives the emergent line strength ratio.

III. MODEL CALCULATIONS

After being modified to include processes described in Section II, the computer code NEBULA (cf., Tarter and Salpeter, 1969; McKee and Tarter, 1975) was used to calculate the radiation field, ionic equilibria, and temperature within a BLR cloud.

These quantities were determined at each point, and then the local excited-state density N_2 was found by solving statistical equilibrium equations involving levels n = 1, 2, and 3, plus the continuum. The cloud was modeled as a static, homogeneous, plane-parallel slab of total column density $N\ell = 10^{23}$ atoms/cm^2, irradiated on one side by photons from a distant source. Gas outside the cloud was assumed to be optically thin to this radiation, which was represented by a single or a multiple power-law spectrum. Specific parameters for different computer runs are listed in Table 2 For comparison, we include a Run S, which is our standard photo-ionization model.

For Run A, the temperature, fractional ionization, and column density are plotted versus Lα optical depth in Fig. 1. The flat portion of the $(N\ell)$ - vs - τ_{21} curve identifies the HII/HI transition region at $\ell \simeq \ell_{uv}$ [cf., Eq. (3)]. Because the behavior of these graphed quantities is similar in all five X-ray models, we conclude that the internal structure of BLR clouds is not sensitive to restricted variations of the metals' concentration, the incident photon spectrum, or the gas density. In particular, lowering the abundances of heavy elements (which are the main source of X-ray opacity) increases the depth to which gas still can be significantly heated and ionized by X-rays, but it has the overall effect of just stretching out the $\ell > \ell_{uv}$ portions of the curves drawn in Fig. 1.

In Fig. 2, we reproduce the radiation continuum at three depths in the multiple-power-law model, Run B;

the (Nℓ) - values 10^{21}, 10^{22}, and 10^{23} cm^{-2} correspond to Lyman continuum optical depths of 3, 10^4, and 10^5. The absorption of successively higher energy X-rays maintains the extensive zone of warm, partially ionized gas that is evident in Fig. 1.

Although there is much similarity in the general structure of BLR clouds with different model parameters, among the Runs A - E there are important differences in relative line strengths. This is clear from an examination of Table 3. A representative QSO emission spectrum compares best with Run E, which has a larger value of the ionization parameter ϕ_{uv}/N than the other models. In each run, though, x-ray heating and ionization decreased the Lα/Hα ratio from the standard run's value of 50, by a factor ranging from 10 to 35. Further, in all runs with solar abundances, the strength of MgII relative to Lα is increased by about a factor of three over the value computed for Run S.

Some details from Runs A and E are also worth noting. The data in Table 4 show that the asymptotic value of the integrated Lα/Hα line strength ratio $J_{21,32}$ is reached at much smaller optical depths in the lower density BLR cloud. This happens because, at a given depth ℓ, the fractional ionization is higher in the lower density case, and proportionally more Hα excitations occur. The tabulated ratios $j_{21}(\tau_{21})/j_{21}(0)$ and $j_{32}(\tau_{21})/j_{32}(0)$, which measure the local change in the production rates of Lyman α and Balmer α radiation, indicate that the low Lα/Hα ratios are caused almost entirely by enchanced Hα emission.

IV. A DISCUSSION OF BLR SPECTRA

A. Dust, and selective destruction of Lyman line radiation

One scheme for reproducing measured hydrogen line ratios within the context of standard, ultraviolet photoionization models involves the selective destruction of Lα photons by dust along the line of sight to the BLR, or within BLR clouds themselves (Netzer and Davidson, 1979; Ferland and Netzer, 1979). However, there now are several observations and arguments which indicate that dust has only a small effect on line ratios and that few Lα photons are destroyed. Baldwin and Netzer (1978) analyzed the (HeII λ 1640)/Lα intensity ratio in 13 high redshift QSO's, and concluded that Lα emission is suppressed by no more than a factor of two in the BLR clouds of any of these objects. Our calculations, shown in Table 3, agree with this conclusion. Furthermore, the conclusion of Baldwin and Netzer is in accord with the fact that the observed ratio of Lα photons to Lyman continuum photons is approximately equal to the estimated covering factor for BLR clouds (cf., Puetter et al., 1979). Yet another relevant point is that measured Balmer decrements do not correlate with optical spectral indices α_{uv} in the manner expected if reddening within the clouds is the cause of the observed steepening (Neugebauer et al., 1979). Altogether, these statements strongly argue that selective destruction of uv line radiation occurs outside the BLR, if at all.

However, the idea of strong external reddening is at odds with the work of McKee and Petrosian (1974), who found that outside our Galaxy the lines of sight to QSO's are essentially dust-free, and with the following observations. The infrared measurement of the Paschen α line in 3C 273 (Grasdalen, 1976), in conjunction with Lα and Hα data, rules out any significant extinction of uv radiation from that QSO. An analogous, but less definite, result was also obtained for the QSO PG 0026 + 129 (Puetter et al., 1978; Baldwin et al., 1978). Moreover, IUE observations of the spectrum of 3C 390.3 (Ferland et al., 1979) reveal that the ratio of strengths of the narrow-line components of Lα and Hα is that expected from recombination theory, and that only the much stronger broad-line components have an anomalously low Lα/Hα ratio. (This measurement is most informative and , if possible, it should be repeated for other objects with known Lyman/Balmer ratios.)

F. X-Rays, and selective enhancement of Balmer line radiation

If few Lyman line photons are destroyed, then Balmer line emission from the BLR clouds must be greatly enhanced in order to explain the low Lα/Hα ratios. This alternative, favored by Baldwin (1977) in his original discussion of the problem, also is suggested by the inability of standard recombination theory--given the observed number of ionizing photons--to account for the observed Balmer line strengths (Baldwin et al., 1978). The most plausible source of enhanced Balmer emission is electron impact excitation of H atoms kept in the n = 2 level by huge

Lα optical depths (cf., Krolik and McKee, 1978). This scheme requires a modest ionization fraction deep within the BLR clouds (where $\tau_{21} > 10^6$), a situation that is not possible in uv ionization models (see, e.g., London, 1979). Recently, though, Canfield and Puetter (1980) argued that low Lyman/Balmer line ratios could be achieved if the radiation transfer in the very thick Lα line were properly treated in these models. Although their comments regarding Lα transfer are valid, the model they propose is highly ionized throughout, and this condition is inconsistent with the observations of broad MgII and FeII lines in QSO and Seyfert spectra (cf., Phillips, 1978; Grandi and Phillips, 1978; Netzer, 1980). In any event, our use of depth-dependent escape probabilities, including partial redistribution for Lα [Eq. (12)], obviates most of their criticism of earlier work.

An important clue as to the importance of X-rays in the enhancement of Balmer line radiation was provided by Elvis et al., (1978), who noticed that the soft X-ray luminosities of Seyfert 1 galaxies correlate with their Hα luminosities, but not with their luminosities in the recombination line HeII λ4686 or in the forbidden lines of O III. Unfortunately, at least for QSO's, there is no strong correlation between Lα luminosity and total optical luminosity (cf., Richstone and Schmidt, 1980). Thus, if QSO's and AGN are similar in regard to both of these relationships, one would not expect to find a correlation between the line intensity ratio Lα/Hα and the luminosity ratio L_{opt}/L_{xr}. This is true for the data compiled in Table I.

Independently of our work, Kwan and Krolik (1979) performed calculations that included absorption of X-rays by BLR clouds. They demonstrated that, at large La optical depths, ionization of excited-state H atoms by the optical continuum keeps the fractional ionization above 15 percent for column densities $N\ell < 10^{21.6}\,cm^{-2}$; concurrently, Balmer line radiation is efficiently pumped by thermal ($T \sim 10^4$K) electron impact excitations from the $n = 2$ level. However, in their model they incorrectly assumed that all the absorbed X-ray energy directly heats electrons in the gas. Our calculations--which include ionizations by nonthermal electrons as well as X-ray heating, but not the excited-state ionizations--therefore are complementary to theirs. A detailed computation incorporating all these effects would allow more accurate predictions, but would be very difficult to accommodate in the NEBULA code. Therefore, we estimated the relative importance of these different ionization schemes by computing the ratio of ionization rates,

$$\varepsilon(\tau_{21}) \equiv \frac{N_2\Gamma_2(\text{optical photons})}{N_1\Gamma_1(\text{nonthermal } e^-)} \approx 10^{3.6}\,\frac{N_2\phi_{uv}}{N_1\phi_{xr}}. \qquad (16)$$

The $\varepsilon(\tau_{21})$ curves for our Runs A and E are plotted in Fig. 3.

Since the ionization fraction is small when ε is large, it follows from Eq. (9) that $x(\varepsilon) \approx x_o(1 + \varepsilon)^{1/2}$, where $x(\varepsilon)$ and x_o are the ionization fractions computed with and without the contribution of excited-state photoionizations. From Fig. 3, we see that only within a restricted range of column density is $x(\varepsilon)$ significantly greater than x_o.

Thus, it is evident that neither ionization mechanism dominates at all depths in a BLR cloud, and that the $N\ell$-values for which $\varepsilon > 1$ depend upon specific model parameters. This result may help explain the uniformity of observed Lyman/Balmer line ratios, since conditions in individual BLR clouds undoubtedly vary, and our computed models and that of Kwan and Krolik yield hydrogen line strengths that are about the same.

C. Other Spectral Features

In addition to the lines that we have discussed, QSOs and Sy 1 galaxies typically show broad, permitted emission lines of He II, He I, O I, and Fe II. Netzer (1980) has argued that the Fe II lines result from collisional excitation in a partially ionized zone similar to the X-ray absorbing zone in our models. Our models give an acceptable intensity for Mg II λ2799 and, within the uncertainties in the relevant photoionization and charge transfer parameters, it seems likely from Netzer's discussion that acceptable Fe II intensities will also result. Our column densities are large enough to produce self absorption in the optical Fe II lines, as required by Phillips (1978) to give the observed relative line strengths. Our success in explaining the Mg II intensity may remove the need to truncate the BLR clouds, which Blumenthal and Mathews (1979) argued was necessary to avoid excessive Mg II emission. In fact, any explanation of the Lα/Hα ratio in terms of enhanced Balmer emission has the consequence of reducing the expected Mg II/Hβ ratio, so that greater MgII lunimosities can be tolerated.

Observed HeII intensities also support the idea of enhanced Balmer line radiation. For recombination line emission only, photoionization by a power law continuum leads to the rather model independent prediction I (λ4686)/I(Hβ) $\approx$ 0.3, whereas lower values are often observed. For example, this ratio is <0.02 in 3C273 (Baldwin 1975). Since the presence of optically thin gas tends to increase this ratio, the low observed values offer strong support for the idea of substantial Balmer line enhancement.

It is more difficult to determine the effects of X-ray heating and ionization on HeI emission. HeI(λ5876) is often quite strong in QSO's and AGN (MacAlpine 1976, Netzer 1978), but the combined scattering and collisional excitation mechanisms proposed by these authors would not be important in our warm, neutral region. However, excitation of the metastable $2\ ^3S$ helium state by non-thermal electrons (resulting from X-ray absorption) may be quite effective, and this could lead to the same kind of enhancement of λ5876 as suggested by MacAlpine and by Netzer.

The OI(λ8446) line, which appears in BLR spectra with an intensity several hundredths that of Hα (Grandi, 1980), is thought to be produced by fluorescent conversion of Lβ photons arising in regions with large Hα optical depths τ_{32} (Shields, 1974). For a solar abundance of oxygen, Netzer and Penston (1976) derived the expression

$$I(\lambda 8446)]/I(H\alpha) = 10^{-4.6} \langle s_{32} \rangle, \qquad (17)$$

where $\langle s_{32} \rangle$ is the mean number of Hα scatterings. Heretofore, in discussions of this problem, a Doppler profile has been assumed for the Hα line shape, with the consequence that $\langle s_{32} \rangle \sim \tau_{32} \sqrt{\ell n \tau_{32}}$. However, it is necessary to take into account the damping wings of the line, and for the Voigt profile (Athay, 1972)

$$\langle s_{32} \rangle = 1/2 \, \pi^{3/4} \sqrt{\tau_{32}/a} \quad , \tag{18}$$

a being the usual Voigt parameter.

For a Doppler half-width of 20 km/s (cf. Netzer, 1980) and natural damping, $a = 0.0024$. We estimated the Hα optical depth from Eqn. (16) by assuming that $\varepsilon \simeq 1/2$ inside the X-ray heated zone. Thus,

$$\frac{\tau_{32}}{\tau_{21}} \approx \frac{N_2 f_{23} \nu_{12}}{N_1 f_{12} \nu_{23}} = 8 \left(\frac{N_2}{N_1}\right) = 10^{-3.0} \left(\frac{\phi_{xr}}{\phi_{uv}}\right) \quad , \tag{19}$$

where the f's are oscillator strengths. Upon collecting results we obtain

$$\frac{I(\lambda 8446)}{I(H\alpha)} = 10^{-4.7} \sqrt{\tau_{21} \phi_{xr} / \phi_{uv}} \quad . \tag{20}$$

The large Lα optical depths computed in our BLR models, $10^8 \leq \tau_{21} \leq 10^9$, together with measured ultraviolet and X-ray fluxes, yield $0.03 \leq I(\lambda 8446)/I(H\alpha) \leq 0.1$, in accord with the observations.

We acknowledge stimulating discussions with G. Ferland, J. Krolik, and H. Netzer. This collaboration was begun when one of us (G.A.S.) was a summer guest at the Lawrence Livermore Laboratory. Our research has been performed under the auspices of the U. S. Department of Energy, and has been supported by DoE contracts DE-AC02-76-CH03073 and W-7405-ENG-48 and NASA grant NSG 7232.

G. A. Shields: Department of Astronomy, RLM 15.212, University of Texas, Austin, TX 78712

C. B. Tarter: Lawrence Livermore Laboratory, P. O. Box 808, Livermore CA 94550

J. C. Weisheit: Princeton Plasma Physics Laboratory, P. O. Box 451, Princeton, NJ 08544

REFERENCES

Athay, R. G. 1972, Radiation Transport in Spectral Lines (D. Reidel: Dordrecht - Holland) §5.

Baldwin, J. A. 1975, Ap. J. 201, 26.

——— 1977, M.N.R.A.S. 178, 67P.

Baldwin, J. A. and Netzer, H. 1978, Ap. J. 226, 1.

Baldwin, J. A., Rees, M. J., Longair, M. S. and Perryman, M. A. C. 1978, Ap. J. (Lett.) 226, L57.

Bergeron, J. and Collin-Souffrin, S. 1973, Aston. Ap. 25, 1.

Blumenthal, G. R. and Mathews, W. G. 1979, Ap. J. 233, 479.

Boggess, A., Daltabuit, E., Torres-Peimbert, S., Estabrook, F. B., Wahlquist, H. D., Lane, A. L., Green, R., Oke, J. B., Schmidt, M., Zimmerman, B., Morton, D. C., and Roeder, R. C. 1979, Ap. J. (Lett.) 230, L131.

Boksenberg, A., Snijders, M. A. J., Wilson, R., Benevenuti, P., Clavell, J., Macchetto, F., Penston, M., Boggess, A., Gull, T. R., Gondhaleker, P., Lane, A. L., Turnrose, B., Wu, C. C., Burton, W. M., Smith, A., Bertola, F., Capaccioli, M., Elvins, A. M., Fosbury, R., Tarenghi, M., Ulrich, M.-H., Hackney, R. L., Jordan, C., Perola, G. C., Roeder, R. C., and Schmidt, M. 1978, Nature 275, 404.

Brown, R. L. and Gould, R. J. 1970, Phys. Rev. D1, 2252.

Butler, S. E., Bender, C. F. and Dalgarno, A. 1979, Ap. J. (Lett.) 230, L59.

Canfield, R. C. and Puetter, R. C. 1980, Ap. J. (Lett.) 236, L7.

Canizares, C. R., McClintock, J. E. and Ricker, G. R. 1978, Ap. J. (Lett.) 226, L1.

Davidson, A. F. 1979, talk presented at I. A. U. Symposium No. 92, "Objects of High Redshift."

Davidson, K. 1977, Ap. J. 218, 20.

Davidson, K. and Netzer, H. 1979, Rev. Mod. Phys. 51, 715.

Elvis, M., Maccacaro, T., Wilson, A. S., Ward, M. J., Penston, M. V., Fosbury, R. A. E. and Perola, G. C. 1978, M. N. R. A. S. 183, 129.

Ferland, G. F. and Netzer, H. 1979, Ap. J. 229, 274.

Ferland, G. F., Rees, M. J., Longair, M. S. and Perryman, M. A. C. 1979, M. N. R. A. S. 187, 65P.

Grandi, S. A. 1980, preprint.

Grandi, S. A. and Phillips, M. M. 1978, Ap. J. 220, 426.

Grasdalen, G. L. 1976, Ap. J. (Lett.) 208, L11.

Habing, H. J. and Goldsmith, D. W. 1971, Ap. J. 166, 525.

Hyland, A. R., Becklin, E. E. and Neugebauer, G. 1978, Ap. J. (Lett.) 220, L73.

Krolik, J. H. and McKee, C. F. 1978, Ap. J. Suppl. 37, 459.

Ku, W. W.-H. 1979, talk presented at the I. A. U. XVII General Assembly (Montreal).

Kwan, J. and Krolik, J. H. 1979, Ap. J. (Lett.) 233, L91.

London, R. 1979, Ap. J. 228, 8.

MacAlpine, G. M. 1976, Ap. J. 204, 694.

McCarroll, R. and Valiron, P. 1976, Astron. Ap. 53, 83.

McKee, C. F. and Petrosian, V. 1974, Ap. J. 189, 17.

McKee, C. F. and Tarter, C. B. 1975, Ap. J. 202, 306.

Mushotzky, R. F., Marshall, F. E., Boldt, E. A., Holt, S. S. and Serlemitsos, P. J. 1980, Ap. J. 235, 377.

Netzer, H. 1978, Ap. J. 219, 822.

——— 1980, Ap. J. 236, 406.

Netzer, H. and Davidson, K. 1979, M.N.R.A.S. 187, 871.

Netzer, H. and Penston, M. V. 1976, M.N.R.A.S. 174, 319.

Neugebauer, G., Oke, J. B.,Becklin, E. E. and Matthews, K. 1979, Ap. J. 230, 79.

Oke, J. B. and Zimmerman, B. 1979, Ap. J. (Lett.) 231, L13.

Otsuka, M. 1979, J. Quant. Spectrosc. Rad. Transfer 21, 489.

Phillips, M. M. 1978, Ap. J. 226, 736.

Puetter, R. C., Smith, H. E., Soifer, B. T., Willner, S. P. and Pipher, J. L. 1978, Ap. J. (Lett.) 226, L53.

Puetter, R. C. Smith, H. E. and Willner, S. P. 1979, Ap. J. (Lett.) 227, L5.

Richstone, D. O. and Schmidt, M. 1980, Ap. J. 235, 361.

Shields, G. A. 1976, Ap. J. 204, 330.

——— 1979, Publ. Astron. Soc. Pacific 91, 618.

Shuder, J. M. and MacAlpine, G. M. 1979, Ap. J. 230, 348.

Shull, J. M. 1979, Ap. J. 234, 761.

Soifer, B. T., Oke, J. B., Matthews, K. and Neugebauer, G. 1979, Ap. J. (Lett.) 227, L1.

Spitzer, L. and Scott, E. H. 1969, Ap. J. 158, 161.

Stark, J. P., Burnell, J. Bell, and Culhane, J. L. 1978, M. N. R. A. S. 182, 23P.

Tananbaum, H., Avni, Y., Branduardi, G., Elvis, M., Fabbiano, G., Feigelson, E., Giacconi, R., Henry, J. P., Pye, J. P., Soltan, A. and Zamorani, G. 1979, Ap. J. (Lett.) 234, L9.

Tarter, C. B. and Salpeter, E. E. 1969, Ap. J. 156, 953.

Watson, W. D. and Christensen, R. B. 1979, Ap. J. 231, 627.

Weisheit, J. C. 1974, Ap. J. 190, 735.

Withbroe, G. 1971, in The Menzel Symposium on Solar Physics, Atomic Spectra, and Gaseous Nebulae, N.B.S. Spec. Pub. 353, ed. K. B. Gebbie (Washington: NBS) 127.

Table 1. Measured Spectral Properties of QSO's and AGN

Object	$\frac{I(L\alpha)}{I(H\alpha)}$	$\frac{I(L\alpha)}{I(H\beta)}$	$\frac{I(H\alpha)}{I(H\beta)}$	$\log\left[\frac{L_{opt}(0.3 - 0.6\mu m)}{erg/s}\right]$	$\left[\frac{L_{xr}(0.5\text{-}5\ keV)}{L_{opt}(0.3 - 0.6\mu m)}\right]$
3C 273	1.8[a]	5.5[a]	3.1[a],6[b]	46.5[c]	1.1[d]
PKS 0237 - 23	1.7[e]	——	——	47.1[c]	——
B2 1225 + 317	0.8[f],0.34[g]	——	6[f]	47.7[h]	0.1[d]
PG 0026 + 129	——	6[i]	4.0[c]	45.2[c]	0.3[d]
<QSO>	——	(3 - 6)[h], ≤ 10[j]	4.4[k]	——	0.8[d]
3C 120	——	4.8[l]	5.1[l]	44.5[m]	0.8[m]
3C 390.3	0.8[n]	4.8[n]	6.1[n]	44.9[m]	0.8[m]
Mrk 79	——	2.2[l]	4.6[l]	44.3[m]	0.3[m]
NGC 4151	——	4.4[b]	3.6[m]	43.1[m]	0.5[m]
<AGN>	——	——	4.2[m]	——	0.3[p]

References to Table 1.

(a) Boggess et al., (1979)

(b) Boksengerg et al., (1978)

(c) Neugebauer et al., (1979)

(d) Tananbaum et al., (1979)

(e) Hyland et al., (1978)

(f) Soifer et al., (1979)

(g) Puetter et al., (1979)

(h) Baldwin (1977)

(i) Puetter et al., (1978), Baldwin et al., (1978)

(j) Richstone and Schmidt (1980)

(k) Shuder and MacAlpine (1979)

(l) Oke and Zimmerman (1979)

(m) Elvis et al., (1978)

(n) Ferland et al., (1979)

(p) Ku (1979)

Table 2 Parameters for BLR Model Calculations

Quantity	Computer Run S	A	B	C	D	E
$\log[\phi_{uv}(cm^{-2}s^{-1})]$	18	18	18	18	17	18
$\log[N(cm^{-3})]$	10	10	10	10	9	9
d_o(pc)	2/3	2/3	2/3	2/3	2	2/3
metals abundance*	solar	solar	solar	$\frac{1}{10}$ solar	solar	solar
spectrum†	1PL	1PL	MPL	1PL	1PL	1PL
ϕ_{xr}/ϕ_{uv}	0	0.026	0.06	0.026	0.026	0.026

*solar abundances from Withbroe (1971).

†1PL denotes a single power-law flux, $\alpha_{uv} = \alpha_{xr} = 1$. MPL denotes $\alpha(\nu \leq 50\nu_H) = 3/2$, $\alpha(50\nu_H \leq \nu \leq 1000\nu_H) = 1/2$, $\alpha(\nu > 1000\nu_H) = 1$.

Table 3 Total, Integrated BLR Line Strengths Relative to Lα = 100.

Line	Computer Run						
	S*	A	B	C	D	E	<QSO>†
HI(λ6563)	2	55	33	36	20	69	77
HeII(λ1640)	3	4	4	3	3	6	5
CIII](λ1909)	3	3	5	1	8	9	18
CIV(λ1549)	21	29	47	15	22	97	40
OVI(λ1034)	1	0.9	0.5	0.3	0.8	35	20
MgII(λ2799)	8	23	25	2	17	34	23

*In this run, only 24% of Lα is from radiative recombination.

†Davidson and Netzer (1979).

Table 4 Local and Integrated Lyman α and Balmer α Line Strength Data

Quantity	$N_\ell(cm^{-2})$ 10^{21}	10^{22}	10^{23}
(Run A)			
τ_{21}	$10^{7.3}$	$10^{8.7}$	$10^{9.8}$
$J_{21,32}$	9.7	2.4	1.8
$j_{21}(\tau_{21})/j_{21}(0)$	$10^{-0.35}$	$10^{-2.6}$	0
$j_{32}(\tau_{21})/j_{32}(0)$	70	90	14
(Run E)			
τ_{21}	$10^{3.5}$	$10^{8.1}$	$10^{9.7}$
$J_{21,32}$	16	1.5	1.5
$j_{21}(\tau_{21})/j_{21}(0)$	1	$10^{-0.34}$	$10^{-2.6}$
$j_{32}(\tau_{21})/j_{32}(0)$	1	41	23

CAPTIONS FOR FIGURES

Fig. 1 Parameters for the BLR cloud of Run A, plotted versus Lα optical depth. $T_4 = 10^{-4}\, T(^oK)$ and $x = N_e/N$.

Fig. 2 The continuum radiation flux computed at different column densities $N\ell(cm^{-2})$ in the BLR Cloud of Run B. The incident flux, identified as the dashed line, is described in Table 2.

Fig. 3 The enhancement factor ε for hydrogen photoionization from excited states (cf. Eqn. 16).

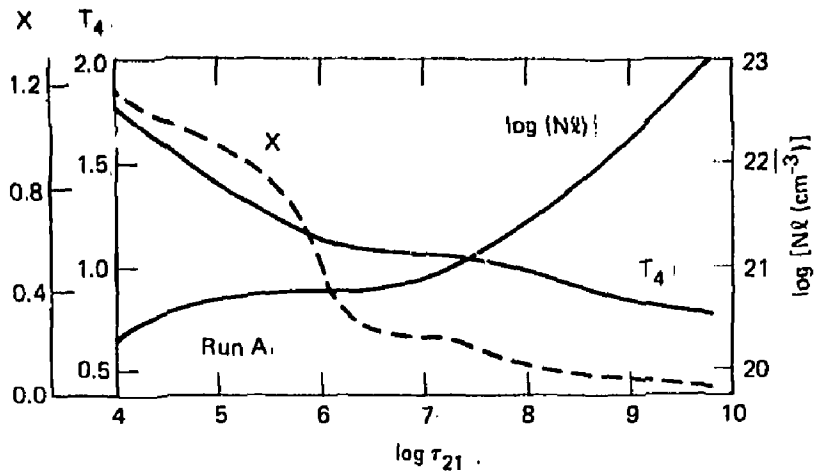
X
T_4
2.0
1.5
1.0
0.5
1.2
0.8
0.4
0.0
X
log (Nℓ)
T_4
Run A
23
22
21
20
log [Nℓ (cm^{-3})]
4
5
6
7
8
9
10
log τ_{21}

Fig. 1.

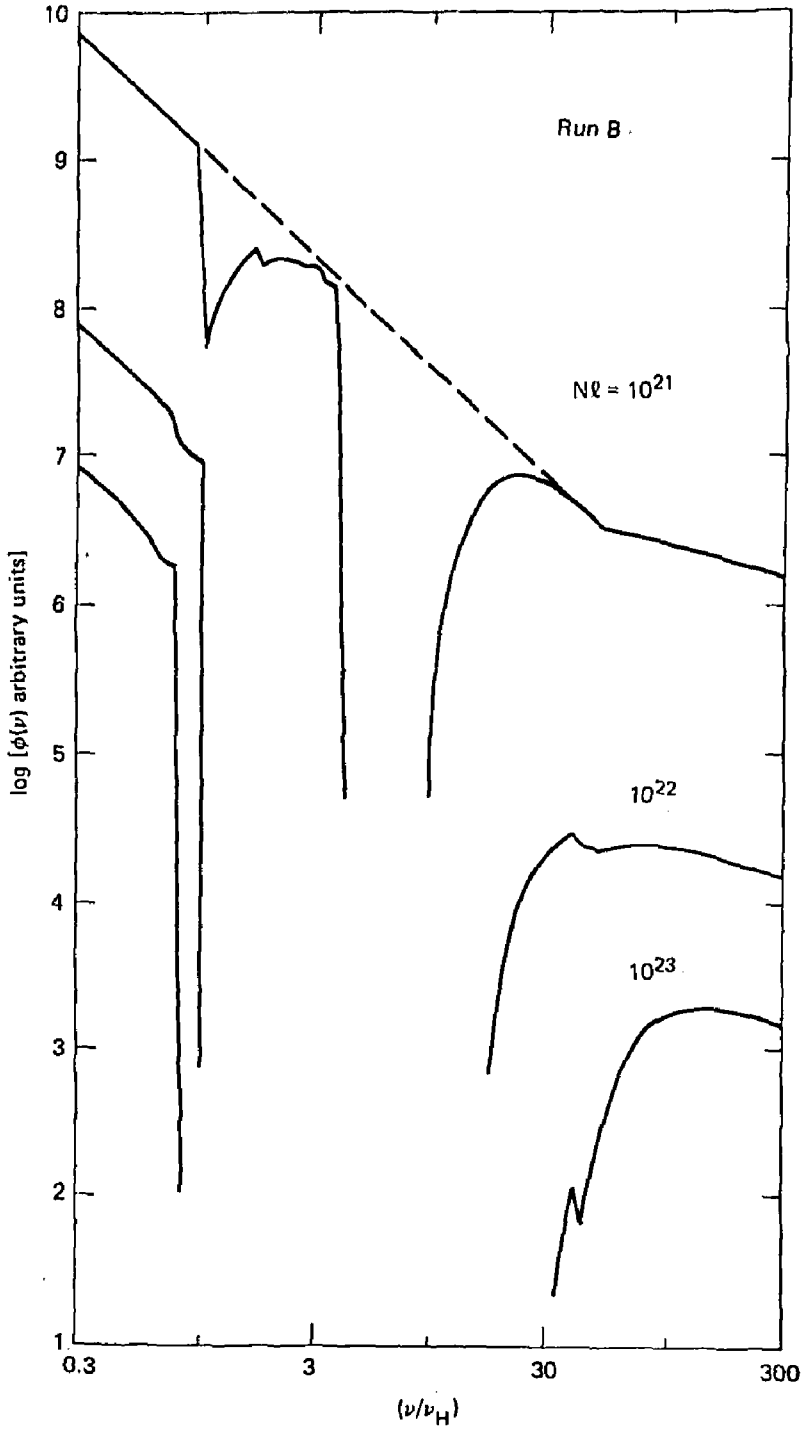
Run B
Nℓ = 10^21
10^22
10^23
log [φ(ν) arbitrary units]
(ν/ν_H)
10
9
8
7
6
5
4
3
2
1
0.3
3
30
300

Fig. 2.

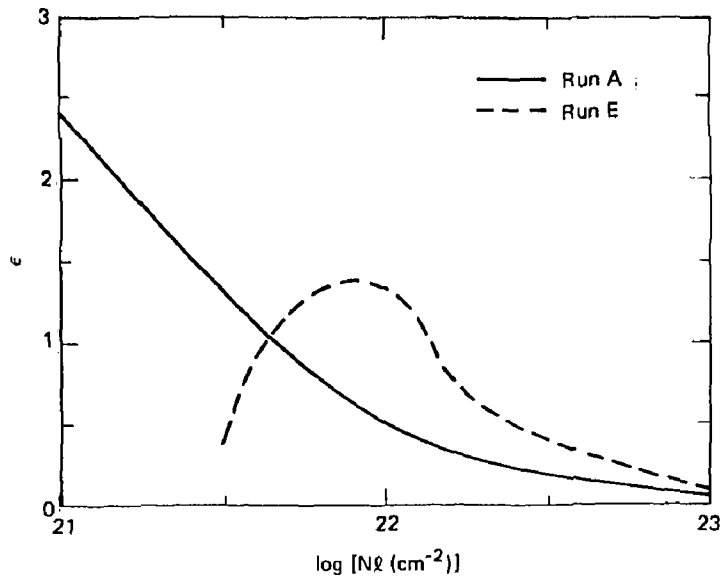

Fig. 3.